nature materials
Vol. 1 No. 4 December 2002
www.nature.com/naturematerials

Lasers probe ultrafast lattice dynamics

POLYMER SYNTHESIS Biological factories

NANOSCALE TRANSISTORS Carbon beats silicon

PROTEIN ARRAYS Chaperones for nanoparticles

Inducing and probing non-thermal transitions in semiconductors using femtosecond laser pulses

Soon after it was discovered that intense laser pulses of nanosecond duration from a ruby laser could anneal the lattice of silicon, it was established that this so-called pulsed laser annealing is a thermal process. Although the radiation energy is transferred to the electrons, the electrons transfer their energy to the lattice on the timescale of the excitation. The electrons and the lattice remain in equilibrium and the laser simply 'heats' the solid to the melting temperature within the duration of the laser pulse. For ultrashort laser pulses in the femtosecond regime, however, thermal processes (which take several picoseconds) and equilibrium thermodynamics cannot account for the experimental data. On excitation with femtosecond laser pulses, the electrons and the lattice are driven far out of equilibrium and disordering of the lattice can occur because the interatomic forces are modified due to the excitation of a large (10% or more) fraction of the valence electrons to the conduction band. This review focuses on the nature of the non-thermal transitions in semiconductors under femtosecond laser excitation.

S. K. SUNDARAM*[1,2] AND E. MAZUR[2]

[1]Pacific Northwest National Laboratory, Richland, Washington 99352, USA
[2]Division of Engineering and Applied Sciences, Harvard University, Cambridge, Massachusetts 02138, USA
*e-mail: sk.sundaram@pnl.gov

Chemical reactions, phase transitions, and surface processes occur on timescales comparable to the natural oscillation periods of atoms and molecules, in the range of femtoseconds (1 fs = 10^{-15} s) to picoseconds (1 ps = 10^{-12} s). Advances in the generation of ultrashort laser pulses in the past two decades[1,2] have made it possible to observe these fundamental processes. These advances have taken us from the picosecond timescale[3–6] a generation ago, to the femtosecond timescale[7–18] in the past decade, and recently into the attosecond (1 as = 10^{-18} s) regime[19–25]. Materials science, interdisciplinary by nature, has benefited from these advances because recent studies[26] — including probing atomistic processes in model materials[9], ultrafast X-ray diffraction of lattices[3] and ultrafast laser processing of materials[26] — are furthering our understanding of time-dependent processes in materials. Femtosecond pulses are ideally suited for studying ultrafast electron and lattice dynamics in semiconductors because they allow observation of the onset of melting, evaporation and ablation in these materials.

ULTRAFAST ELECTRON AND LATTICE DYNAMICS

On excitation with an ultrashort pulse, a semiconductor undergoes several stages of relaxation before returning to equilibrium. The energy is transferred first to the electrons and then to the lattice. The interaction includes several regimes of carrier excitation and relaxation. We can distinguish the following four regimes: (1) carrier excitation, (2) thermalization, (3) carrier removal and (4) thermal and structural effects[10]. These regimes and the timescales for the corresponding processes are shown in Fig. 1. The triangles at the top of the figure mark the current state-of-the-art in the generation of ultrashort pulses of various wavelengths. In the visible region, pulses as short as 5 fs allow direct probing of carrier dynamics down to the shortest timescales (triangle 1). Diffraction of hard X-ray pulses of 200 fs duration (triangle 2) permit observation of structural and atomic rearrangements in the bulk of materials, but not the carrier excitation and carrier–lattice interaction processes that precede the structural dynamics, because X-rays cannot see electrons. The shortest pulses obtained to date, of 800-as duration (triangle 3), are in the soft X-ray region, and are limited to probing core-level transitions in excited atoms.

Figure 2 illustrates some of the processes that take place in the four regimes of Fig. 1 for a typical direct-gap semiconductor[10]. The various processes shown do not occur sequentially; they overlap in time, forming a

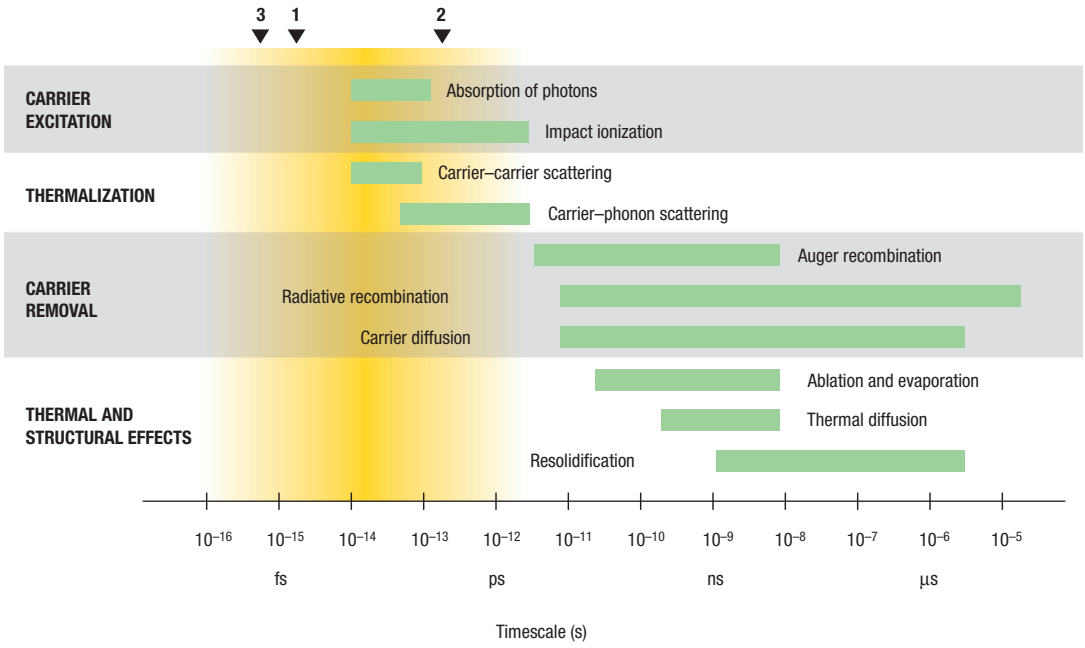

Figure 1 Timescales of various electron and lattice processes in laser-excited solids (after ref. 10). Each green bar represents an approximate range of characteristic times over a range of carrier densities from 10^{17} to 10^{22} cm^{-3}. The triangles at the top show the current state-of-the-art in the generation of short pulses of electromagnetic radiation: **1** 5 fs (visible), **2** 120 fs (X-ray), **3** 0.5 fs (far ultraviolet).

continuous chain of events spanning the entire range from femtoseconds to microseconds. For example, carriers thermalize at the same time as they cool by transferring energy to lattice phonons. Non-thermal structural effects (for example formation of transient structures) can occur while the lattice is still cold. Various mechanisms of the electron and lattice dynamics through the four major regimes are elaborated on in this section, and highlighted in Fig. 2.

CARRIER EXCITATION

When the photon energy is larger than the bandgap, single photon absorption (Fig. 2a, left) is the dominant mechanism for exciting valence electrons to the conduction band. In the case of semiconductors with an indirect bandgap, such as silicon, single photon absorption can still occur with photons of energy greater than the gap, but phonon assistance is necessary to conserve momentum. Multiphoton absorption (Fig. 2a, right) is important if the direct gap is greater than the photon energy, especially in transparent insulators, or if the single photon absorption is inhibited by band filling.

In solids, scattering causes rapid dephasing of the coherence between the excitation and the electromagnetic field that causes it. For GaAs, the dephasing time is between 3.5 and 11 fs (ref. 12). Consequently, coherent effects — oscillation of electron–hole pairs between the valence and conduction bands — are only observed on a timescale of 10 to 100 fs. Boltzmann kinetics, which describe the overall electron and hole distributions and the effects of scattering on them, is not valid in this regime[27,28]. Only after this coherence is lost are the carriers really free.

Free carrier absorption (Fig. 2b) increases the energy of carriers in the electron–hole plasma or that of the initially free electrons in a metal. Although this absorption increases the energy of the free carrier population, it does not alter its number density. However, if some of the carriers are excited well above the bandgap (or Fermi level in a metal), impact ionization (Fig. 2c) can generate additional excited carriers.

THERMALIZATION

After excitation, electrons and holes are redistributed throughout the conduction and valence bands by carrier–carrier and carrier–phonon scattering. Carrier–carrier scattering (Fig. 2d) is a two-body process (an electrostatic interaction between two carriers), which does not change the total energy in the excited carrier system or the number of carriers. Carrier–carrier scattering can cause dephasing in less than 10 fs, but it takes hundreds of femtoseconds for the carrier distribution to approach a Fermi–Dirac distribution. In a carrier–phonon scattering process, free carriers lose or gain energy and momentum by emission or absorption of a phonon. The carriers remain either in the same conduction or valence band valley (intravalley scattering, Fig. 2e) or transfer to a different valley (intervalley scattering, Fig. 2f). Although carrier–phonon scattering does not change the number of carriers, their energy decreases due to spontaneous phonon emission, which transfers energy to the lattice. In metals and semiconductors, carrier–carrier and carrier–phonon scattering occur concurrently during the first few hundred femtoseconds after excitation. Because the emitted phonons carry little energy, it takes many scattering processes, and therefore several picoseconds, before the carriers and the lattice reach thermal equilibrium.

CARRIER REMOVAL

Once the carriers and the lattice are in equilibrium, the material is at a well-defined temperature. Although the carrier distribution has the same

temperature as the lattice, there is an excess of free carriers compared to that in the thermal equilibrium. The excess carriers are removed either by recombination of electrons and holes or by diffusion out of the excitation region.

During radiative recombination, the inverse of the optical excitation process, the excess carrier energy is given up in the form of a photon (luminescence, Fig. 2g). Non-radiative recombination processes include Auger recombination, and defect and surface recombination. During Auger recombination, an electron and a hole recombine and the excess energy excites an electron higher in the conduction band (Fig. 2h). Like other recombination mechanisms, Auger recombination decreases the carrier density. However, it keeps the total energy in the free carrier system constant, and the average energy of the remaining carriers increases. In defect and surface recombination, the excess energy is given to a defect or surface state. Carrier diffusion removes carriers from the region of the sample where they were originally excited (Fig. 2i) and so, in contrast to recombination processes, it does not decrease the total number of free carriers in the material. In semiconductors, carrier confinement due to a decrease in bandgap on the excitation of a high carrier density[4], slows down the diffusion away from the photoexcited region. This laser-induced bandgap renormalization has been confirmed by theory[29] as well as by experimental results[30].

THERMAL AND STRUCTURAL EFFECTS

When the free carriers and the lattice come to an equilibrium temperature and the excess free carriers have been removed, the material is essentially the same as that heated by conventional means. Material excited by ultrashort laser pulses can achieve the equilibrium temperature in just a few picoseconds, but the removal of excess carriers takes longer. If the lattice temperature exceeds the melting or boiling point, melting or vaporization can occur, but not on the picosecond timescale. The material is superheated but remains solid until regions of liquid or gas nucleate. Starting from nucleation sites at the surface, the liquid and/or gas phase expands into the material (Fig. 2j). As the energy deposited by the laser pulse is converted to kinetic energy of the lattice ions, individual atoms, ions, molecules or clusters can leave the surface, leading to ablation (Fig. 2k, that is, not thermal evaporation). Thermal diffusion limits expansion of the liquid region by cooling the photoexcited region. If no phase transition occurs, the temperature reverts back to the ambient value on the timescale of microseconds. If melting or vaporization has occurred, then resolidification (Fig. 2l) or condensation ensues as the temperature falls below the melting or boiling points, respectively; however, the material does not necessarily revert back to its original structure or phase[31,32].

THERMAL AND NON-THERMAL STRUCTURAL TRANSITIONS

Laser-induced annealing in semiconductors has generated extensive debate since the late 1970s. Some suggestions have been made that sufficiently dense photoexcited plasma could weaken the lattice, giving atoms enhanced mobility without significantly increasing their thermal energy (the so-called plasma-annealing model)[33,34]. In disagreement with this model, it was shown[5] that a simple thermal model can account for observed changes in the reflectivity of pico- and nanosecond laser-excited Si, Ge and GaAs (ref. 6).

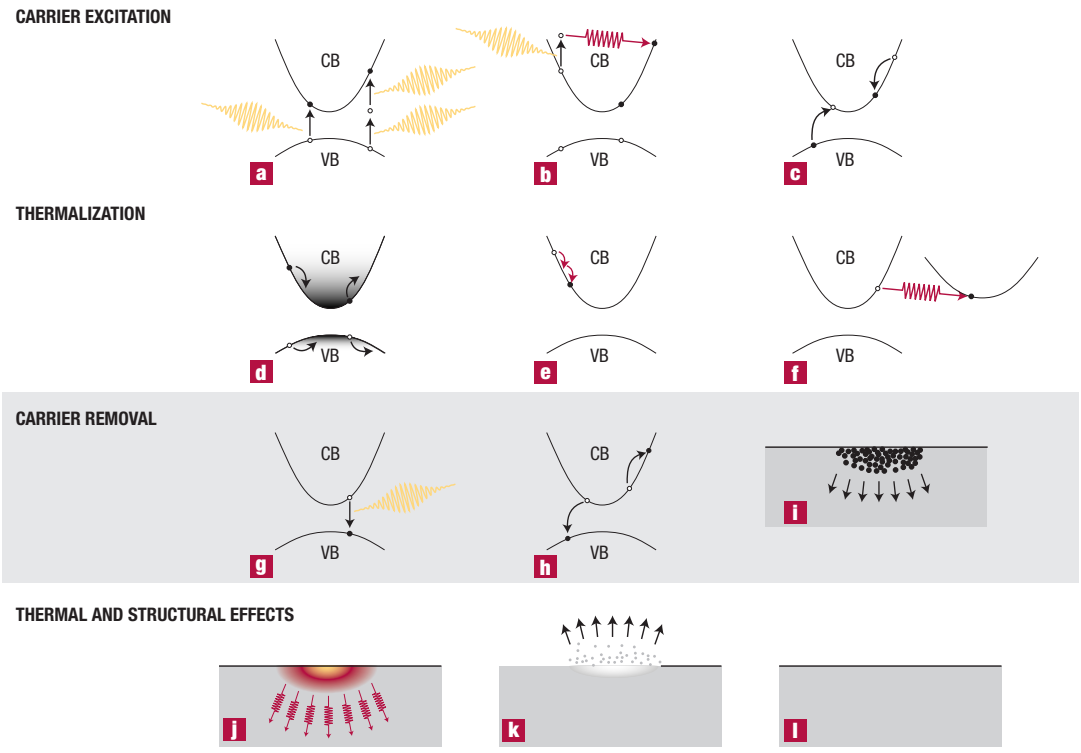

Figure 2 Electron and lattice excitation and relaxation processes in a laser-excited direct gap semiconductor. CB is the conduction band and VB the valence band. **a**, Multiphoton absorption. **b**, Free-carrier absorption. **c**, Impact ionization. **d**, Carrier distribution before scattering. **e**, Carrier–carrier scattering. **f**, Carrier–phonon scattering. **g**, Radiative recombination. **h**, Auger recombination. **i**, Diffusion of excited carriers. **j**, Thermal diffusion. **k**, Ablation. **l**, Resolidification or condensation.

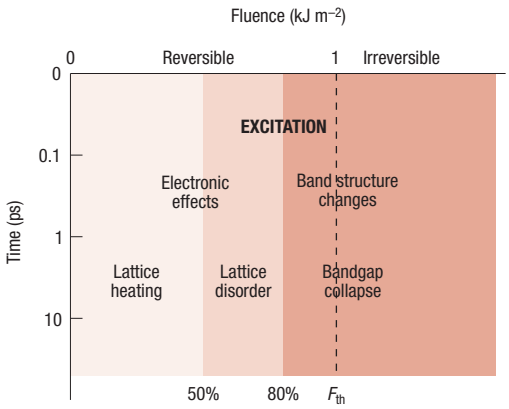

Figure 3 Summary of the electronic and structural dynamics in GaAs on excitation with short laser pulses (after ref. 10). Excitations range from 0.1 to 2.0 kJ m^{-2}. Three shaded regions indicate three distinct regimes.

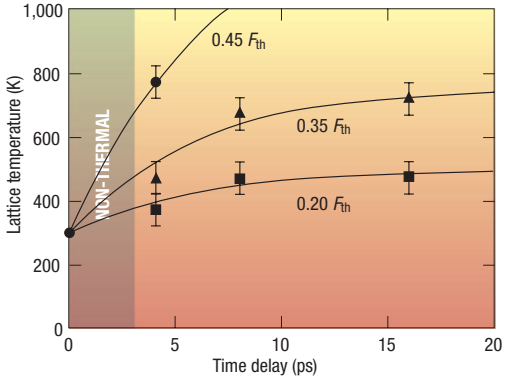

Figure 4 Laser-induced lattice heating of crystalline GaAs at three different excitations below the threshold for irreversible changes F_{th}. Exponential curve-fitting yields a common rise time of about 7 ps for lattice heating. (After ref. 49.)

The model assumes that the excess energy of photoexcited electrons relaxes within the duration of the excitation pulse to the lattice vibrational modes by emission of longitudinal optical phonons. The lattice heats to the melting temperature, and as the latent heat of fusion is supplied, the material melts. Because thermalization of the absorbed optical energy takes only a few picoseconds, the thermal model works well for any material that is excited with laser pulses of picosecond or longer duration[13–15].

For picosecond and subpicosecond laser pulses, however, ample experimental evidence exists from Shank and co-workers[16] and other groups, that non-thermal structural changes can be driven directly by electronic excitation[17,33–39]. According to the so-called non-thermal plasma model, the lattice is disordered by direct excitation of the electronic system, while the lattice modes remain vibrationally cold[18,40,41]. Absorption of photons creates a free carrier plasma and, when about 10% of valence electrons are removed from bonding orbitals, the lattice is weakened. Photoexcitation can thus give the atoms enhanced mobility without increasing their thermal energy. The non-thermal model assumes that the rate of phonon emission by the excited electronic system is slow compared with the laser pulse duration. When this assumption is satisfied, and a large enough fraction of the valence electrons is excited, structural change can occur while the electronic system and the lattice are not in thermal equilibrium with each other, although each of these systems may internally be in quasi-equilibrium.

TECHNIQUES OF FEMTOSECOND MATERIALS SCIENCE

New developments in experimental femtosecond techniques have greatly advanced our knowledge of non-thermal laser-induced structural changes. Whereas most experiments use optical probing of the electronic structure of materials, the recent realization of subpicosecond X-ray pulses is beginning to make possible direct probing of the lattice during a structural transition.

Most measurements involving subpicosecond laser pulses are variations on the so-called pump–probe scheme. A laser pulse (the pump) excites the material to be studied, creating an initial condition and defining a zero in time. A second laser pulse (the probe) measures the response of the material to the excitation. By varying the time delay between the arrivals of the pump and the probe pulses at the sample, the time evolution of the response can be measured. Various optical probing techniques exist for studying the response to the excitation. These include time-resolved measurements of reflectivity or transmission, of luminescence or Raman emission, of surface or bulk second-harmonic generation, and time-resolved ellipsometry measurements of the dielectric function.

Because optical probing only couples to the electronic system, information on lattice structural changes must be inferred indirectly from changes in the electronic system. A sensitive probe of lattice structural changes is provided by the second-order susceptibility $\chi^{(2)}$ of a material because this quantity reflects the symmetry of the system. A detector measures the radiation at the second-harmonic frequency $2\omega_o$ generated by the probe beam in the material. For a centrosymmetric material, such as silicon[42–44], $\chi^{(2)}$ vanishes in the bulk and only the surface contributes to $\chi^{(2)}$ (ref. 42). When the material undergoes a structural transition, the value of $\chi^{(2)}$ changes, providing a way for probing the dynamics of these transitions. Surface reflectivity and second-harmonic measurements at a single angle of incidence indicate that the surface of silicon loses its cubic order in 150 fs after excitation with a 100 fs pulse, that is, well before the lattice heats up[44].

For non-centrosymmetric materials such as GaAs, $\chi^{(2)}$ is nonzero in the bulk; when the material disorders, $\chi^{(2)}$ vanishes and so the second-harmonic signal is a sensitive probe of the loss of order on melting or excitation. The measured second-harmonic signal depends not only on the second-order susceptibility $\chi^{(2)}$, but also on the linear optical properties. Therefore the dielectric constant at the fundamental and second-harmonic frequencies, $\varepsilon(\omega_o)$ and $\varepsilon(2\omega_o)$ must be known so that $|\chi^{(2)}|$ can be extracted from the data. The dielectric constant $\varepsilon(\omega_o)$ at the fundamental frequency determines the intensity and orientation of the probe beam inside the sample, and the amount of second-harmonic signal propagating out of the sample depends on $\varepsilon(2\omega_o)$.

Second-harmonic measurements[31,45–48], combined with two-angle reflectivity measurements[5,6,13–15,32,33,39]

of the linear optical properties at both the fundamental and second-harmonic in GaAs show different regimes[31]: (1) at low fluences (< 0.5 kJ m^{-2}), $\chi^{(2)}$ exhibits a partial drop, followed by a recovery to its initial value within a few picoseconds, (2) at medium fluences (0.8–1.0 kJ m^{-2}), $\chi^{(2)}$ drops to zero but recovers to its initial value in some hundreds of nanoseconds, and (3) at high fluences above the threshold of irreversible changes of 1.0 kJ m^{-2}, $\chi^{(2)}$ vanishes and never recovers to its initial value. The vanishing of $\chi^{(2)}$ does not necessarily mean that the material has taken on a true centre of inversion within each unit cell, but indicates that the material has lost order on lengthscales up to the optical wavelength. As the data show, the GaAs permanently loses its order on this lengthscale above the threshold for irreversible changes. Interestingly, just below this threshold, the lattice also disorders for hundreds of nanoseconds before regaining its original non-centrosymmetric structure.

Information on the changes in band structure that accompany laser-induced structural changes have been obtained from direct measurement[10] of the dielectric function across a broad range of frequencies in the visible spectrum. The dielectric function is a sensitive probe of the electron dynamics and provides information on the state the material (for example, solid or liquid, ordered or disordered). Time-resolved broadband ellipsometry measurements of the dielectric function of a variety of materials has yielded a wealth of information on laser-induced structural transitions[6]. Data are obtained by measuring the reflectivity of a broadband continuum pulse[33] at two angles of incidence and numerically inverting the Fresnel equations. Figure 3 summarizes the findings of extensive measurements of the dielectric function of GaAs on excitation by femtosecond laser pulses[49–55]. Like the data on $\chi^{(2)}$, the results fall in three distinct regimes of excitation. At low excitation fluence, below 0.5 kJ m^{-2} (or about 50% of the threshold for irreversible structural change, F_{th}), the free carriers scatter from the central valley (around minima where crystal momentum $k = 0$) to the side valleys in less than 500 fs. The carriers relax by rapid Auger recombination and phonon emission, causing the lattice to heat in about 7 ps; the higher the fluence, the higher the temperature of the lattice (Fig. 4). At intermediate fluences, between 50% and 80% of threshold fluence F_{th}, the initial electronic effects on $\varepsilon(\omega)$ are stronger and less easy to interpret. The excited carriers influence the dielectric function through a combination of free-carrier absorption, band filling, and changes in the band structure due to ionic screening and other many-body effects. The data are consistent with models describing superheating[56], amorphization[57] and the formation of a liquid layer[58], but it is not possible to determine which model applies. After about 4 ps, however, the dielectric function takes on the shape of that of amorphous GaAs, indicating that the lattice has undergone a non-thermal order–disorder transition. Above 80% of threshold fluence F_{th} the data show a clear semiconductor-to-metal transition with a gradual closing of the bandgap over a timescale of several picoseconds (or hundreds of femtoseconds at higher fluences). The transition is non-thermal because the changes start and finish well before carrier-lattice thermalization is complete. In agreement with the second-harmonic data, the dielectric function shows a reversible order–disorder transition just below the threshold for permanent damage. Femtosecond time-resolved microscopy also indicates a non-thermal electronic transition at high fluence[59,60].

Picosecond X-ray pulses have been used to observe the generation and propagation of coherent acoustic pulses in bulk GaAs (ref. 3) and the non-thermal disordering of Ge (ref. 61). The recent realization of subpicosecond X-ray pulses makes it possible to directly probe fast atomic-scale motions[62]. These pulses have been used to study multilayer laser-heated organic films[63] and Ge–Si heterostructures[64]. In Si and GaAs, non-thermal disordering has been observed by optical measurements at excitation fluences greater than 1.5 times the damage threshold[48,58]. Just above the threshold, disordering takes tens of picoseconds, consistent with a thermal melting process.

Like GaAs, InSb undergoes a structural transition on the picosecond timescale at sufficiently high laser fluence[65–67]. In contrast to GaAs, however, the transition is from a zinc-blende structure to a centrosymmetric metastable state[65]. The observed rapid changes in reflectivity and in second-harmonic signal support an electron–hole plasma-assisted solid-to-solid phase transition rather than a thermal transition. Recent ultrafast time-resolved X-ray diffraction shows a decrease in diffracted X-ray intensity in as little as 350 fs

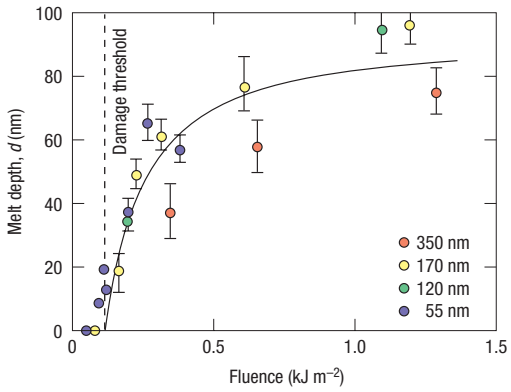

Figure 5 Thickness of the molten layer as function of the absorbed laser fluence. Femtosecond X-ray measurements allow the determination of the thickness *d* of the molten layer developing on top of InSb exposed to ultrashort visible laser pulses at X-ray wavelengths between 55 and 350 nm. (After ref. 68.)

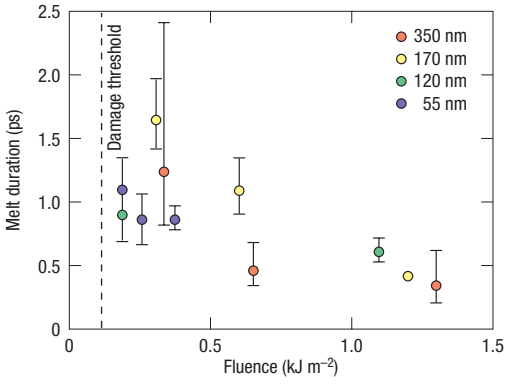

Figure 6 Duration of the melting process as a function of the absorbed laser fluence. The time it takes to disorder the InSb lattice can be obtained from the decrease in the femtosecond X-ray diffraction intensity measured at X-ray wavelengths between 55 and 350 nm. (After ref. 68.)

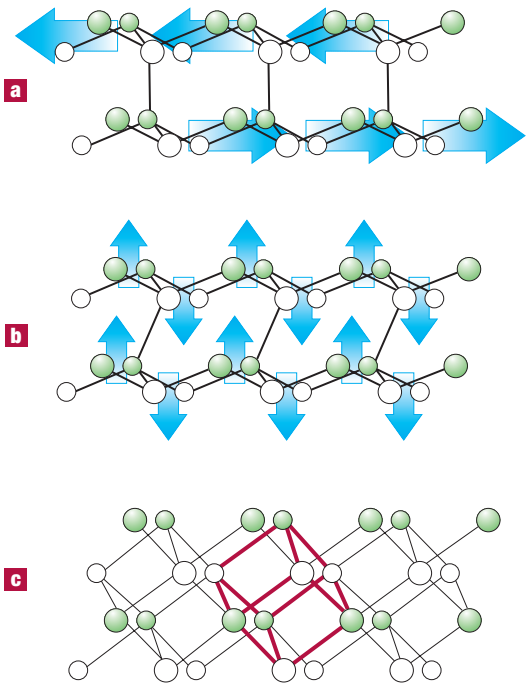

Figure 7 Illustration of structural changes in the diamond structure of GaAs induced by longitudinal and transverse distortions. **a**, Ideal diamond structure. The arrows show the transverse acoustic distortion. **b**, Intermediate structure due to the transverse acoustic distortion. The arrows show the longitudinal optical distortion. **c**, The two distortions lead to a new structure containing fragments of a simple cubic structure (shown in red). (After ref. 74.)

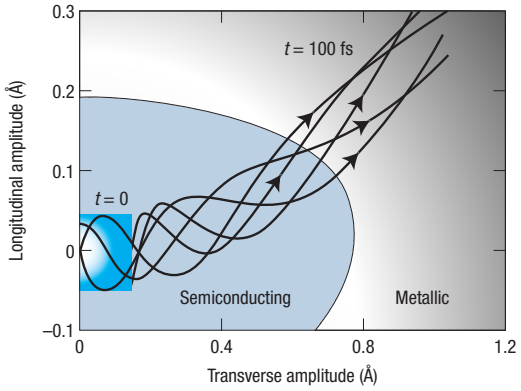

Figure 8 Evolution of a diamond lattice during the first 100 fs after the excitation of a dense electron–hole plasma. Before the laser pulse, the crystal is at room temperature and the lattice executes oscillations within the rectangular blue-shaded region. Five possible trajectories resulting from numerical solutions of the equation of motion are shown for $t > 0$. In less than 100 fs the trajectories enter a region where the gap between the valence and conduction band has vanished, resulting in metallic properties. (After ref. 74.)

(ref. 68). Although the longitudinal optical phonon emission time is only 200 fs, it takes many longitudinal optical phonon emissions (and therefore several picoseconds) to transfer all the excess energy from the electrons to the lattice. In addition, the observed decrease in X-ray diffraction intensity is too large to be explained by a thermal Debye–Waller effect[69]. Analysing the data in terms of a simplified model of a disordered or liquid layer of thickness d on top of an unperturbed solid, yields the values of d shown in Fig. 5. Figure 6 shows the corresponding time for the diffraction intensity to decrease. Higher fluence results in larger d and thus the faster disordering process. The solid line through the data in Fig. 5 is a fit to a simple model that assumes that melting occurs to a depth d if the intensity at that point exceeds a critical value. The critical intensity obtained from this fit is approximately equal to the threshold for irreversible surface damage determined from post-mortem analysis of the samples. The fact that the time constant for disordering exceeds 1 ps just above the damage threshold suggests the existence of an energy barrier that must be surmounted for the non-thermal transition to occur. At higher fluence, less time is required to cross the barrier and so the transition occurs more quickly.

MODELLING

Ab initio calculations and empirical treatments of high-density phases of semiconductors have shown that Si undergoes a transition under hydrostatic compression from its diamond structure to a β-tin structure due to an elastic instability[70,71]. The instability of the diamond and zinc-blende structures under intense laser pulse excitation has been modelled by analysing lattice distortions caused by phonons and then examining the effect of the electron–hole plasma on the cohesive energy of the diamond structure[72–76]. The dense electron–hole plasma causes an instability[72] of both the transverse acoustic phonons[73] and the longitudinal optical phonons[74] in Si. Earlier phenomenological bond-charge models[75,76], that do not account for the repulsive force due to a laser-induced electron–hole plasma, and that therefore do not include distortions due to longitudinal optical phonons, underestimate the instability due to transverse acoustic phonons. Figure 7 shows how these transverse and longitudinal distortions act in harmony to cause a transition from a semiconducting to a metallic phase[74]. The calculations show that in GaAs, the presence of a dense electron–hole plasma causes the zinc-blende structure to become unstable and change into a centrosymmetric metallic phase on a subpicosecond timescale (Fig. 8), in agreement with experimental observations[33,39,53]. To make a transition to a centrosymmetic phase, the relative distance between planes of the structure must change (Fig. 7b,c), and so the transition must involve longitudinal optical phonons at the central valley where the crystal momentum $k = 0$ (Γ point)[74].

The dielectric function of pulsed-laser excited GaAs has been modelled using an approach that combines *ab initio* electronic structure calculations with non-equilibrium quantum many-body physics[77]. By assuming that the ions are fixed in their lattice positions and that the electrons and holes have relaxed to the band extrema, this model explores the changes that occur in the linear optical properties before ion motion. In agreement with the experimental observations, the model predicts a reduction in the height of the main resonance peak of the dielectric function.

Simulations using tight-binding electron–ion dynamics of the electronic and structural response of GaAs to ultrashort laser pulses show features that are fully consistent with time-resolved measurements of the dielectric function[78–80]. The calculations show that when 10% of the valence electrons are excited into the conduction band, the ions perform large excursions from their initial positions causing permanent structural change. Accompanying this structural transition, the calculations predict a collapse of the bandgap, as has been observed experimentally.

CONCLUSION

There are two ways in which a laser pulse can destabilize the structure of a molecule or material: on the picosecond or longer timescale, the energy of the electrons that are excited by the laser is transferred to thermal motion of the ions. On the subpicosecond timescale, the excitation of a large fraction of electrons from bonding to anti-bonding states causes the repulsive interatomic forces to immediately disorder the lattice. This means that excitation with pulses of duration of several picoseconds or longer lead to a completely thermal solid–liquid melting transition. For pulses of subpicosecond duration, however, the material disorders non-thermally—that is, before the lattice has equilibrated with the carriers.

Over the last decade both femtosecond optical and X-ray measurements have unambiguously shown that such non-thermal order–disorder transitions can occur, sometimes even below the threshold for permanent structural change. At the same time, computational materials science has begun to provide a detailed microscopic understanding of the behaviour of electrons and ions when a semiconductor is irradiated with a short intense laser pulse. Experiments and simulations have shown that covalently bonded lattices become unstable when about 10% of the valence electrons are excited to the conduction band and that this instability leads to the very rapid disordering of the lattice.

Current experiments focus on a better understanding of the nature of the disordered transient phases that appear on excitation. In many cases, these transient phases are metal-like disordered or glassy phases. A better understanding of these phases may lead to schemes for optically 'controlling' the electronic and structural state of a material. Despite all the rapid advances in this exciting new field, many challenges remain. Improvements in both the intensity and time-resolution of pulses in the X-ray regime will increase our understanding of the motion of the ions during optically induced transitions. Further increasing the fluence of visible femtosecond laser pulses might make it possible to induce purely electronic—and therefore nearly instantaneous—phase transitions. For example, a semiconductor could take on a metallic character while the lattice is still undisturbed, providing a femtosecond optical switch. The wealth of new data on femtosecond laser-induced transitions spurred on by the rapid advances in experimental capabilities provides new opportunities in modelling. Detailed modelling of the lattice changes that occur in optically induced transitions could, for example, significantly advance our understanding of these transitions. As the experimental and computational tools further improve, we can also expect a plethora of new applications ranging from ultrafast optical switching in optical signal processing, to new materials for read–write optical data storage and integrated opto-electronic circuits.

doi: 10.1038/nmat767

References

1. Shank, C. V. in *Ultrashort Laser Pulses – Generation and Applications* (ed. Kaiser, W) 5–34 (Springer, Berlin and New York, 1993).
2. Hirlimann, C. in *Femtosecond Laser Pulses – Principles and Experiments* (ed. Rullière, C.) 83–110 (Springer, Berlin, 1998).
3. Rose-Petruck, C. *et al.* J. Picosecond-milliångstrom lattice dynamics measured by ultrafast X-ray diffraction. *Nature* **398,** 310–312 (1999).
4. van Driel, H. M. Kinetics of high-density plasmas generated in Si by 1.06- and 0.53-μm picosecond laser pulses. *Phys. Rev. B.* **35,** 8166–8176 (1987).
5. Liu, P. L., Yen, R. & Bloembergen, N. Picosecond laser-induced melting and resolidification morphology on Si. *Appl. Phys. Lett.* **34,** 864–866 (1979).
6. Wang, J.-K., Saeta, P., Buijs, M., Malvezzi, M. & Mazur, E. in *Ultrafast Phenomena VI* (eds Yajma, T., Yoshihara, K., Harris, C. B. & Shionoya, S.) 236–239 (Springer, Berlin, 1989).
7. Balistreri, M. L. M., Gersen, H., Korterik, J. P., Kuipers, L. & van Hulst, N. F. Tracking femtosecond laser pulses in space and time. *Science* **295,** 1080–1082 (2001).
8. Stapelfeldt, H., Constant, E. & Corkum. P. B. Femtoscience: from femtoseconds to attoseconds. *Prog. Cryst. Growth Charact.* **33,** 209–215 (1996).
9. Zewail, A. H. Femtochemistry: Atomic-scale dynamics of the chemical bond. *J. Phys. Chem. A* **104,** 5660–5694 (2000).
10. Callan, J. P. in *Ultrafast Dynamics And Phase Changes In Solids Excited By Femtosecond Laser Pulses* 59–104 Thesis, Harvard Univ., Cambridge, (2000).
11. Callan, J. P., Kim, A. M.-T., Roeser, C. A. D., Mazur, E. Ultrafast dynamics and phase changes in highly excited GaAs. *Semiconduct. Semimet.* **67,** 151–203 (2001).
12. Becker, P. C. *et al.* Femtosecond photon echoes from band-to-band transitions in GaAs. *Phys. Rev. Lett.* **61,** 1647–1649 (1988).
13. Wang, J.-K., Saeta, P., Buijs, M. & Mazur, E. in *Nonlinear Optics and Ultrafast Phenomena* (eds Alfano, R. R. & Rothberg, L. J.) 61–64 (Nora, New York, 1990).
14. Wang, J.-K., Saeta, P., Siegal, Y., Mazur, E. & Bloembergen, N. in *Ultrafast Phenomena VI* (eds Harris, C. B., Ippen, E. & Zewail, A. H.) 321–323 (Springer, Berlin, 1990).
15. Wang, J.-K. *Femtosecond Nonlinear Optics In Gases And Solids* Thesis, Harvard Univ., Cambridge, (1992).
16. Shank, C. V., Yen, R. & Hirlimann, C. Time-resolved reflectivity measurements of femtosecond-optical-pulse-induced phase transitions in silicon. *Phys. Rev. Lett.* **50,** 454–457 (1983).
17. Lowndes, D. H. & Jellison, G. E. Jr. in *Semiconductors and Semimetals* Vol. 23 (eds Wood, R. F., White, C. W. & Young, R. T.) 313–404 (Academic, Orlando, 1984).
18. Van Vechten, J. A., Tsu, R., Saris, F. W. & Hoonhout, D. Reasons to believe pulsed laser annealing of Si does not involve simple thermal melting. *Phys. Lett. A* **74,** 417–421 (1979).
19. Corkum, P. B. Attosecond pulses at last. *Nature* **403,** 845–846 (2000).
20. Paul, P. M. *et al.* Observation of a train of attosecond pulses from high harmonic generation. *Science* **292,** 1689–1692 (2001).
21. Drescher, M. *et al.* X-ray pulses approaching the attosecond frontier. *Science* **291,** 1923–1927 (2001).
22. Silberberg, Y. Physics at the attosecond frontier. *Nature* **414,** 494–495 (2001).
23. Hentschel, M. *et al.* Attosecond metrology. *Nature* **414,** 509–513 (2001).
24. Papadogiannis, N. A., Witzel, B., Kalpouzos, C. & Charalambidis, D. Observation of attosecond light localization in higher order harmonic generation. *Phys. Rev. Lett.* **83,** 4289–4292 (1999).
25. Papadogiannis, N. A. *et al.* Reply. *Phys. Rev. Lett.* **87,** 109402 (2001).
26. Symposium Q, MRS Spring Meeting, 2001. Femtosecond materials science and technology. *Mater. Res. Soc. Bull.* **26,** 560-571 (2001).
27. Bányai, L. *et al.* Exciton-KLO-phonon quantum kinetics: Evidence of memory effects in bulk GaAs. *Phys. Rev. Lett.* **75,** 2188–2191 (1995).
28. Bar-Ad, S. & Chemla, D. S. Quantum kinetics regime during and immediately after laser excitation of semiconductors. *Mater. Sci. Eng. B.* **48,** 83–87 (1997).
29. Zimmerman, R. in *Many Particle Theory of Highly Excited Semiconductors* (eds Eberling, W., Meiling, W., Uhlmann, A. & Wilhelmi, B.) 5–86 (Teubner-Texte zur Physik, Leipzig, 1988).
30. Kalt, H. & Rinker, M. Band-gap renormalization in semiconductors with multiple inequivalent valleys. *Phys. Rev. B.* **45,** 1139–1154 (1992).
31. Glezer, E. N., Siegel, Y., Huang, L. & Mazur, E. The behavior of chi^2 during laser-induced phase transitions in GaAs. *Phys. Rev. B.* **51,** 9589–9596 (1995).
32. Solis, J., Afonso, C. N., Trull, J. F. & Morilla, M. C. Fast crystallizing GeSb alloys for optical data storage. *J. Appl. Phys.* **75,** 7788–7794 (1994).
33. Siegal, Y., Glezer, E. N. & Mazur, E. Dielectric constant of GaAs during subpicosecond laser-induced phase transition. *Phys. Rev. B* **49,** 16403–16406 (1994).
34. Siegal, Y., Glezer, E. N., Huang, L. & Mazur, E. Laser-induced phase transitions in semiconductors. *Annu. Rev. Mater. Sci.* **25,** 223–247 (1995).
35. Malvezzi, A. M., Kurz, H. & Bloembergen, N. in *Energy Beam-Solid Interactions and Transient Thermal Processing* (eds Biegelsen, D. K., Rozgonyi, G. A. & Shank, C. V.) 75–80 (The Materials Research Society, Pittsburgh, 1985).
36. Downer, M. C. & Shank, C. V. Ultrafast heating of silicon on sapphire by femtosecond optical pulses. *Phys. Rev. Lett.* **56,** 761–764 (1986).
37. Malvezzi, A. M. in *Excited-State Spectroscopy in Solids* (eds Grassano, U. M. & Terzi, N.) 335–354 (North-Holland Physics, Amsterdam, 1987).
38. Preston, J. S., van Driel, H. M. & Sipe J. E. Order-disorder transitions in the melt morphology of laser-irradiated silicon. *Phys. Rev. Lett.* **58,** 69–72 (1987).
39. Saeta, P., Wang, J.-K., Siegal, Y., Bloembergen, N. & Mazur, E. Ultrafast electronic disordering during femtosecond laser melting of GaAs. *Phys. Rev. Lett.* **67,** 1023–1026 (1991).
40. Van Vechten, J. A., Tsu, R. & Saris, F. W. Nonthermal pulsed laser annealing of Si; Plasma annealing. *Phys. Lett. A* **74,** 422–426 (1979).

41. von der Linde, D. in *Resonances – A Volume in Honor of the 70th Birthday of Nicolaas Bloembergen* (eds Levinson, M. D., Mazur, E., Pershan, P. S. & Shen, Y. R.) 337–347 (World Scientific, Singapore, 1990).
42. Shank, C. V., Yen, Y. & Hirlimann, C. Femtosecond-time-resolved surface structural dynamics of optically excited silicon. *Phys. Rev. Lett.* **51,** 900–902 (1983).
43. Tom, H. W. K., Heinz, T. F. & Shen, Y. R. Second-harmonic reflection from silicon surfaces and its relation to structural symmetry. *Phys. Rev. Lett.* **51,** 1983–1986 (1983).
44. Tom, H. W. K., Aumiller, G. D. & Briti-Cruz, C. H. Time-resolved study of laser-induced disorder of Si surfaces. *Phys. Rev. Lett.* **60,** 1438–1441 (1988).
45. Govorkov, S. V., Shumay, I. L., Rudolph, W. & Schröder, T. Time-resolved second-harmonic study of femtosecond laser-induced disordering of GaAs surfaces. *Opt. Lett.* **16,** 1013–1015 (1991).
46. Govorkov, S. V., Emelyanov, V. I., Koroteev, N. I. & Shumay, I. L. Femtosecond dynamics of laser-induced phase-transition of the GaAs surface layer to a centrosymmetric phase. *J. Lumin.* **53,** 153–158 (1992).
47. Govorkov, S. V., Schröder, T., Shumay, I. L. & Heist, P. Transient gratings and second-harmonic probing of the phase transformation of a GaAs surface under femtosecond laser irradiation. *Phys. Rev. B* **46,** 6864–6868 (1992).
48. Sokolowski-Tinten, K., Bialkowski, J. & von der Linde, D. Ultrafast laser-induced order-disorder transitions in semiconductors. *Phys. Rev. B* **51,** 14186–14198 (1995).
49. Siegal, Y., Glezer, E. N. & Mazur, E. Dielectric constant of GaAs during subpicosecond laser-induced phase transition. *Phys. Rev. B* **49,** 16403–16406 (1994).
50. Glezer, E. N., Siegal, Y., Huang, L. & Mazur, E. Laser-induced bandgap collapse in GaAs. *Phys. Rev. B* **51,** 6959–6970 (1995).
51. Glezer, E. N., Huang, L., Siegal, Y., Callan, J. P. & Mazur, E. in *Proc. Mater. Res. Soc. Symp.* Vol. 397 (Eds Singh, R., Norton, D., Laude, L., Narayan, J. & Cheung, J.) 3–20 (The Materials Research Society, Pittsburgh, 1995).
52. Glezer, E. N. *et al.* Three-dimensional optical storage inside transparent materials. *Opt. Lett.* **21,** 2023–2025 (1996).
53. Huang, L., Callan, J. P., Glezer, E. N. & Mazur, E. GaAs under ultrafast excitation: response of the dielectric function. *Phys. Rev. Lett.* **80,** 185–188 (1998).
54. Callan, J. P., Kim, A. M. –T., Huang, L. & Mazur, E. Ultrafast electron and lattice dynamics in semiconductors at high excited carrier dynamics. *Chem. Phys.* **251,** 167–179 (2000).
55. Callan, J. P., Kim, A. M.-T., Roeser, C. A. D. & Mazur, E. Universal dynamics during and after ultrafast laser-induced semiconductor-to-metal transitions. *Phys. Rev. B* **64,** 073201–073204 (2001).
56. Blakemore, J. S. Semiconducting and other major properties of gallium arsenide. *J. Appl. Phys.* **53,** R123–R181 (1982).
57. Erman, M., Theeten, J. B., Chambon, P., Kelso, S. M. & Aspnes, D. E. Optical properties and damage analysis of GaAs single crystals partly amorphized by ion implantation. *J. Appl. Phys.* **56,** 2664–2671 (1984).
58. Sokolowski-Tinten, K., Bialkowski, J. & von der Linde, D. Two distinct transitions in ultrafast solid-liquid phase transformations of GaAs. *Appl. Phys. A* **53,** 227–234 (1991).
59. von der Linde, D., Sokolowski-Tinten, K. & Bialkowski, J. Laser-solid interaction in the femtosecond time regime. *Appl. Surf. Sci.* **109/110,** 1–10 (1997).
60. Sokolowski-Tinten, K., Bialkowski, J., Boing, M., Cavalleri, A. & von der Linde, D. Thermal and non-thermal melting of gallium arsenide after femtosecond laser excitation. *Phys. Rev. B.* **58,** R11805–R11808 (1998).
61. Siders, C. W. *et al.* Detection of non-thermal melting by ultrasfast X-ray diffraction. *Science* **286,** 1340–1342 (1999).
62. Schoenlein, R. W. *et al.* Femtosecond X-ray pulses at 0.4 Å generated by 90° Thomson scattering: A tool for probing the structural dynamics of materials. *Science* **274,** 236–238 (1996).
63. Rischel, C. *et al.* Femtosecond time-resolved X-ray diffraction from laser-heated organic films. *Nature* **390,** 490–492 (1997).
64. Sokolowski-Tinten, K. *et al.* Femtosecond X-ray measurement of ultrafast melting and large acoustic transients. *Phys. Rev. Lett.* **87,** 225701 (2001).
65. Shumay, I. L. & Höfer, U. Phase transformations of an InSb surface induced by strong femtosecond laser pulses. *Phys. Rev. B* **53,** 15878–15884 (1996).
66. Chin, A. H. *et al.* Ultrafast structural dynamics in InSb probed by time-resolved X-ray diffraction. *Phys. Rev. Lett.* **83,** 336–339 (1999).
67. Lindenberg, A. M. *et al.* Time-resolved X-ray diffraction from coherent phonons during a laser-induced phase transition. *Phys. Rev. Lett.* **84,** 111–114 (2000).
68. Rousse, A. *et al.* Nonthermal melting in semiconductors measured at femtosecond resolution. *Nature* **410,** 65–68 (2001).
69. Vetelino, J. F. & Gaur, S. P. & Mitra, S, S. Debye-Waller factor for zinc-blende-type crystals. *Phys. Rev. B* **5,** 2360–2366 (1972).
70. Crain, J. *et al.* Theoretical study of high-density phases of covalent semiconductors. I. *Ab initio* treatment. *Phys. Rev. B* **49,** 5329–5340 (1994).
71. Clark, S. J., Ackland, G. J. & Crain, J. Theoretical study of high-density phases of covalent semiconductors. II. Empirical treatment. *Phys. Rev. B* **49,** 5341–5352 (1994).
72. Stampfli, P. & Bennemann, K. H. Theory for the instability of the diamond structure of Si, Ge, and C induced by a dense electron–hole plasma. *Phys. Rev. B* **42,** 7163–7173 (1990).
73. Stampfli, P. & Bennemann, K. H. Dynamical theory of the laser-induced lattice instability of silicon. *Phys. Rev. B* **46,** 10686–10692 (1992).
74. Stampfli, P. & Bennemann, K. H. Time dependence of the laser-induced femtosecond lattice instability of Si and GaAs: Role of longitudinal optical distortions. *Phys. Rev. B* **49,** 7299–7305 (1994).
75. Martin, R. M. Dielectric screening model for lattice vibrations of diamond-structure crystals. *Phys. Rev.* **186,** 871 (1969).
76. Heine, V. & Van Vechten, J. A. Effect of electron–hole pairs on phonon frequencies in Si related to temperature dependence of bandgaps. *Phys. Rev. B* **13,** 1622–1626 (1976).
77. Benedict, L. X. Dielectric function for model of laser-excited GaAs. *Phys. Rev. B* **63,** 075202 (2001).
78. Stampfli, P. & Bennemann, K. H. Theory for the laser-induced femtosecond phase transition of silicon and GaAs. *Appl. Phys. A* **60,** 191–196 (1995).
79. Silvestrelli, P. L., Alavi, A., Parrinello, M. & Frenkel, D. *Ab initio* molecular dynamics simulation of laser melting of silicon. *Phys. Rev. Lett.* **77,** 3149–3152 (1996).
80. Graves, J. S. & Allen, R. E. Response of GaAs to fast intense laser pulse. *Phys. Rev. B* **58,** 13627–13633 (1999).

Acknowledgements

Collaboration between the authors was made possible with support from the Department of Energy under the Environmental Management Science Program. We thank C. A. D. Roeser for a careful review of the manuscript and many helpful comments. S.K.S. acknowledges the support from the Pacific Northwest National Laboratory (PNNL) while writing this review. Battelle Memorial Institute operates PNNL for the United States Department of Energy under Contract DE-AC06-76RLO 1830.

Correspondence and requests for materials should be addressed to S.K.S.

Competing financial interests

The authors declare that they have no competing financial interests.